Structural Studies on Bismuth–Iodide–Hexamethylphosphoramide Complexes by X-Ray Crystallography and Extended X-Ray Absorption Fine Structure Spectroscopy†

William Clegg,[a] Louis J. Farrugia,[b] Andrew McCamley,[a] Nicholas C. Norman,*[,a] A. Guy Orpen,*[,c] Nigel L. Pickett[a] and Susan E. Stratford[c]

[a] *Department of Chemistry, The University of Newcastle upon Tyne, Newcastle upon Tyne NE1 7RU, UK*
[b] *Department of Chemistry, The University of Glasgow, Glasgow G12 8QQ, UK*
[c] *School of Chemistry, The University of Bristol, Cantock's Close, Bristol BS8 1TS, UK*

The reaction between BiI_3 and one equivalent of hmpa [$OP(NMe_2)_3$, hexamethylphosphoramide] in toluene solution affords the neutral orange complex $[Bi_2I_6(hmpa)_2]$ which has been characterised by X-ray crystallography. It exists in the solid state as a polymer of dimers in which a linear chain of weakly interacting Bi_2I_6 units is flanked on either side by hmpa ligands. An analogous reaction between BiI_3 and five equivalents of hmpa in toluene also affords this complex together with small amounts of yellow $[Bi_2I_6(hmpa)_4]$. It is also formed in the reaction between BiI_3 and one equivalent of hmpa in thf (tetrahydrofuran) solution (the X-ray quality crystals were obtained from this solvent), although an additional dark orange, ionic compound $[BiI_2(hmpa)_4][I_3]$ is also formed together with small quantities of black crystalline $[BiI_2(hmpa)_4][I_5]$. The complex $[BiI_2(hmpa)_4][I_3]$ is the major product from the reaction between BiI_3 and five equivalents of hmpa in thf, and was also characterised by X-ray crystallography. The bismuth atom in the cation is co-ordinated by two iodines and four hmpa ligands with an octahedral geometry in which the iodines are mutually *trans*. The factors affecting whether this or the alternative *cis* geometry is adopted are discussed. The nature of $[BiI_2(hmpa)_4][I_5]$ was established from a partial X-ray diffraction data solution and microanalytical data, and further support for this formulation was obtained from solid-state extended X-ray absorption fine structure (EXAFS) spectroscopic data, an analysis of which was consistent with the presence of the cation $[BiI_2(hmpa)_4]^+$. The EXAFS data in thf solution are consistent with a three-co-ordinate bismuth environment with dissociation of most or all of the hmpa ligands.

Bismuth trihalides are appreciably Lewis acidic and readily form adducts with a variety of Lewis bases, a feature which is manifest both in the structures of the halides themselves, and in the many examples of halogenoanions which are known.[1] In so doing, the co-ordination number around the bismuth centre increases, as a result of the presence of halide bridges, from three to four, five or six, the lone pair of electrons in the latter case usually being stereochemically inactive (or nearly so). There are far fewer structural data available, however, for neutral complexes of the general formula $[BiX_3(L)_n]$ where X is halide and L is a neutral two-electron donor ligand. Much of the work which has been reported involves sulfur ligands, and several such complexes have been described by Battaglia and Pelizzi and co-workers. These include the rather complex and disordered salt $[Bi(tu)_6][BiCl_6]\cdot[BiCl_3(tu)_3]$ (tu = thiourea) in which the neutral species $[BiCl_3(tu)_3]$ **1** has a *fac* configuration,[2] $[Bi_2Cl_6(L)_4]$ **2** [L = 1-allyl-3-(2-pyridyl)-thiourea-*S*],[3] the chloride-bridged polymeric species $[\{BiCl_3(L)_2\}_x]$ **3** (L = imidazolidine-2-thione-*S*),[4] *mer*-$[BiCl_3(L)_3]$ **4** [L = 1-phenyl-3-(2-pyridyl)thiourea-*S*],[5] $[Bi_2Cl_6(L)_4]$ **5** (L = *N*,*N*′-diethylimidazolidine-2-thione-*S*),[5] and *mer*-$[BiBr_3(L)_3]$ **6** (L = imidazolidine-2-thione-*S*).[6] More recently, we have reported the first structurally characterised example of a neutral bismuth halide–phosphine complex, $[Bi_2Br_6(PMe_3)_4]$ **7**,[7] together with the mixed phosphine–phosphine oxide species $[Bi_2Br_6(PMe_2Ph)_2(OPMe_2Ph)_2]$ **8**.[7] Two other compounds have also been characterised by X-ray crystallography, namely the phosphine oxide adduct $[Bi_2I_6(OPPh_3)_4]$ **9**[8] and the arsine oxide complex $[Bi_2I_6(OAsPh_3)_3]$ **10**.[9]

From a structural point of view, the mononuclear complexes with the formula $[BiX_3(L)_3]$ adopt either a *fac* structure, as in **1**, or a *mer* geometry as found in **4** and **6**. For complexes with two ligands per bismuth centre, $BiX_3(L)_2$, a dimeric, edge-shared, bioctahedral structure is found for compounds **2**, **5**, **7**, **8** and **9** with the particular centrosymmetric configuration shown in **A**; we have commented previously on the differences between this structure and those observed for the related transition-metal(III) dimers of the form $[M_2X_6(L)_4]$ where X is halide and L is a phosphine,[7] a point to which we will return in a future

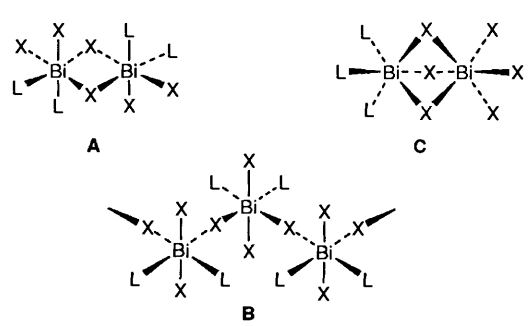

† *Supplementary data available:* see Instructions for Authors, *J. Chem. Soc., Dalton Trans.*, 1993, Issue 1, pp. xxiii–xxviii.

publication. The only exception to a dimeric structure for a $BiX_3(L)_2$ compound is found in **3** which is polymeric with linear chloride bridges as shown in **B**.[4] Complex **10** is the sole example with the empirical formula $BiX_3(L)_{1.5}$, and has a face-shared, bioctahedral structure with three bridging halides and all three ligands (L) bonded to the same bismuth as shown in **C**.

Herein we describe the nature of the products obtained from reactions between bismuth triiodide, BiI_3, and the phosphine oxide hmpa [$OP(NMe_2)_3$, hexamethylphosphoramide] in toluene or thf (tetrahydrofuran) solutions and comment on the structural types observed. Analogous reactions with antimony triiodide, SbI_3, are also described.

Results and Discussion

The reaction between BiI_3 and one equivalent of hmpa in toluene solution resulted in the formation of an orange solution from which an orange solid precipitated over a period of 12 h, microanalytical data for which were consistent with the formulation BiI_3(hmpa) **11**. Compound **11** was also formed when the reaction was carried out in thf solution, although appreciable quantities of dark orange crystals and smaller amounts of black crystals were also formed the nature of which will be discussed later.

The solid-state structure of **11** was established by X-ray crystallography (carried out on crystals obtained from thf–hexane), the results of which are shown in Figs. 1 and 2. Selected bond lengths and angles are shown in Table 1 and atomic positional parameters are presented in Table 2. The essential structural unit of **11** is the crystallographically centrosymmetric dimer $[Bi_2I_6(hmpa)_2]$ (Fig. 1) in which each bismuth is bonded to one hmpa ligand and four iodines. Two iodines, I(2) and I(2a), on each bismuth centre, Bi and Bi(a), are bridging, and fairly symmetrically bonded to each bismuth [Bi–I(2) 3.197(1), Bi–I(2a) 3.119(1) Å] with the hmpa ligands lying in the $Bi_2(\mu\text{-}I)_2$ plane each *cis* to one bridging iodine and *trans* to the other. Both I(3) and I(3a) are perpendicular to this $Bi_2(\mu\text{-}I)_2$ plane (and *trans*) and are terminal with no close contacts to any other bismuth centres which results in this Bi–I bond being the shortest [Bi–I(3) 2.878(1) Å]. The iodines I(1) and I(1a) lie in the $Bi_2(\mu\text{-}I)_2$ plane *cis* to the hmpa ligands and *trans* to I(2) and I(2a) respectively, but are not terminal since they are involved in weak bridging interactions with adjacent bismuth centres, Bi(b) in the case of I(1) [Bi(b)–I(1) 3.400(1) Å], in neighbouring dimeric units. This probably accounts for the slightly longer Bi–I bond length [Bi–I(1) 2.984(1) Å] compared to I(3). The iodine corresponding to I(1) on Bi(b), I(1b), is bonded to Bi such that it is *trans* to I(3) thereby resulting in overall octahedral co-ordination around Bi. Thus, each bismuth centre is bonded to five iodines in total, one of which is terminal, two of which are fairly symmetrically bridging [I(2) and its symmetry related partner] and two of which are very asymmetrically bridging [I(1) and its symmetry related partner]; in this latter case, one of the Bi–I distances is much longer than the other four. The result is a structure which may be described as a polymer of dimers and this is shown in Fig. 2. Furthermore, each $Bi_2(\mu\text{-}I)_2$ bridging unit (symmetric or asymmetric) is perpendicular to its two adjacent bridging units which results in a one-dimensional polymer with hmpa ligands, one per bismuth, alternating on either side of the $\{Bi_2I_6\}_x$ chain.

There are no analogous complexes of the type BiX_3L with which to compare the structure of **11**, but the terminal and bridging Bi–I bond distances are similar to those found in a number of phenyl bismuth iodide and iodobismuthate anion structures (refs. 10 and 11 and refs. therein), and clearly reveal

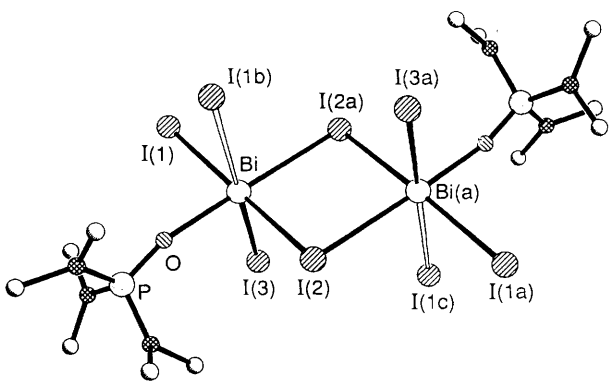

Fig. 1 A view of the centrosymmetric dimeric unit of **11** showing the atom-numbering scheme and the weakly bonded iodine atoms from adjacent dimer units

Table 1 Selected bond lengths (Å) and angles (°) for **11**

Bi–I(1)	2.984(1)	Bi–I(2)	3.197(1)
Bi–I(2a)	3.119(1)	Bi–I(3)	2.878(1)
Bi–I(1b)	3.400(1)	Bi–O	2.295(7)
P–O	1.479(8)		
I(1)–Bi–I(2)	170.9(1)	I(1)–Bi–I(2a)	93.1(1)
I(1)–Bi–I(3)	94.9(1)	I(2)–Bi–I(2a)	89.3(1)
I(2)–Bi–I(3)	93.9(1)	I(2a)–Bi–I(3)	91.9(1)
I(1)–Bi–O	91.8(2)	I(2)–Bi–O	85.2(2)
I(2a)–Bi–O	173.1(2)	I(3)–Bi–O	92.5(2)
Bi–I(2)–Bi(a)	90.7(1)	Bi–O–P	165.4(5)

Atoms labelled a are related by the symmetry operation $1 - x, -y, 1 - z$.

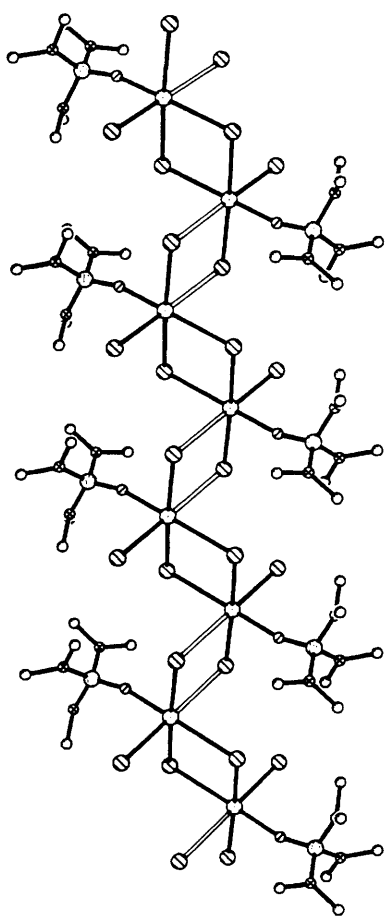

Fig. 2 A view of part of the polymeric solid-state structure of **11**

Table 2 Atomic coordinates ($\times 10^4$) for **11**

Atom	*x*	*y*	*z*
Bi	7 434.0(5)	1 068.1(3)	5 051.8(2)
I(1)	10 430.2(9)	1 316.3(6)	4 265.6(4)
I(2)	4 617.3(10)	531.4(7)	6 047.2(4)
I(3)	5 638.1(11)	3 090.8(7)	4 474.5(5)
P	9 377(3)	2 948(2)	6 501(1)
O	8 852(9)	2 092(7)	5 956(4)
N(1)	10 809(12)	2 357(8)	7 071(5)
N(2)	7 781(13)	3 405(10)	6 890(6)
N(3)	10 199(14)	4 080(8)	6 187(5)
C(11)	10 740(30)	1 150(10)	7 250(10)
C(12)	12 102(17)	3 010(15)	7 509(8)
C(21)	6 206(19)	3 885(16)	6 466(9)
C(22)	7 510(20)	3 080(20)	7 550(10)
C(31)	11 354(19)	3 924(13)	5 697(8)
C(32)	9 950(30)	5 250(10)	6 410(10)

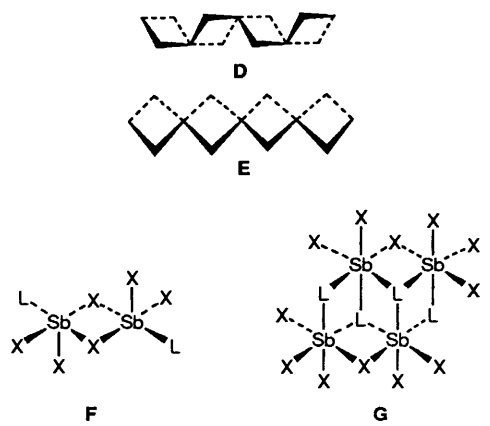

the correlation between primary and secondary bond distances which we and others have noted before (see refs. 10–12 and refs. therein). The structure of the complex $BiPhI_2(thf)$ **12**[10] does, however, provide for an interesting comparison. Complex **12** has a stoichiometry of the form $BiX_3(L)$ analogous to **11**, but where one of the X groups is phenyl rather than iodide. Nevertheless, the structure of **12** is quite similar to **11** in that it comprises a polymeric bismuth iodide backbone with thf ligands on either side as shown in Fig. 3 (see also Figs. 3 and 4 in ref. 10). The main difference between the two structures is that each adjacent pair of bismuth atoms is bridged by two iodines in **11** whereas only one is present in **12**, but the phenyl groups in **12** can also be considered as bridging in that, although they are σ bonded to only one bismuth, there is a weak π interaction to the neighbouring bismuth centre. This bridging phenyl arrangement is also found in the bromide and chloride analogues of **12**, and is discussed in more detail in ref. 11, but if the bridging phenyls in **12** were replaced by bridging iodines, the structure would be similar to that of **11** with thf ligands instead of hmpa except that in **11**, the hmpa ligands are *cis* to the terminal iodines whereas in **12** the thf ligands are *trans* to the terminal iodines. This is clear in Figs. 2 and 3 respectively, and results in the $Bi_2(\mu\text{-}X)_2$ backbones having geometries as illustrated in **D** and **E** for **11** and **12** respectively.

We also draw attention to three related antimony halide compounds with the empirical formula $SbX_3(L)$ described by Pohl *et al.*[13] In contrast to **11**, the structures of $SbBr_3(SPPh_3)$ and $SbI_3(SePPh_3)$ are dimeric as shown in **F**, whereas $SbBr_3(SPMe_2Ph)$ exists as a tetramer with μ- and μ_3-$SPMe_2Ph$ ligands as illustrated in **G**. In both the type **F** compounds, there is an interaction between a phenyl group of the $S/SePPh_3$ ligand and the vacant octahedral site.

As a final point, we note that the Bi–O bond length [2.295(7) Å] in **11** is fairly short which indicates that the hmpa is quite strongly bound to the bismuth centre. Bismuth–oxygen bond lengths for comparison are given in ref. 10 and lie in the range *ca.* 2.0–2.9 Å, but we note that in the various structures in which thf is co-ordinated to a bismuth halide centre, the Bi–O distances are significantly longer being in the range 2.589–2.813 Å.[10,11]

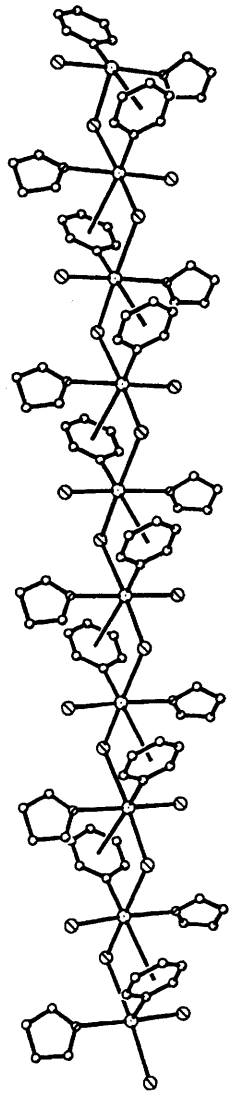

Fig. 3 A view of the polymeric structure of **12**[10]

The reaction between BiI_3 and five equivalents of hmpa in toluene also afforded an orange solution from which an orange powder precipitated. The precipitate was isolated and dissolved in fresh toluene on warming, and combined with the supernatant liquid. Solvent diffusion from an Et_2O overlayer afforded an orange oil, but a crystalline solid product was obtained after dissolution of the orange oil in CH_2Cl_2 and solvent diffusion from a hexane overlayer. This crystalline solid was not homogeneous, however, and consisted of orange crystalline **11** as the major product together with smaller amounts of a yellow material. Crystals of the yellow compound were not suitable for X-ray crystallography, but microanalytical data were consistent with the formula $BiI_3(hmpa)_2$. We suspect that this compound is likely to be dimeric in the solid state with a type **A** structure analogous to **2**, **5**, **7**, **8** and **9**, *viz.* $[Bi_2I_6(hmpa)_4]$ **13**.

The dark orange crystals mentioned above, obtained when the reaction between BiI_3 and one equivalent of hmpa was carried out in thf solution, were isolated as the major crystalline product from the reaction between BiI_3 and five equivalents of hmpa in thf; small quantities of black crystals were again

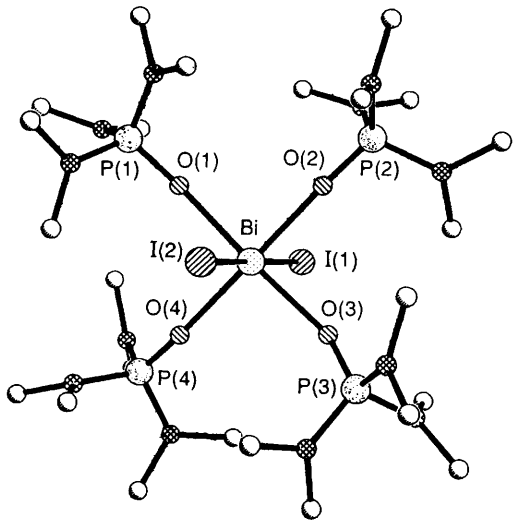

Fig. 4 A view of the cation $[BiI_2(hmpa)_4]^+$ in **14** (**14a**)

Table 3 Selected bond lengths (Å) and angles (°) for **14**

Bi–I(1)	3.069(2)	Bi–I(2)	3.034(2)
Bi–O(1)	2.340(8)	Bi–O(2)	2.305(9)
Bi–O(3)	2.327(9)	Bi–O(4)	2.351(9)
P(1)–O(1)	1.499(9)	P(2)–O(2)	1.490(10)
P(3)–O(3)	1.490(9)	P(4)–O(4)	1.488(10)
I(1)–Bi–I(2)	176.43(3)	I(1)–Bi–O(1)	92.6(2)
I(1)–Bi–O(2)	89.1(2)	I(1)–Bi–O(3)	88.0(2)
I(1)–Bi–O(4)	89.2(2)	I(2)–Bi–O(1)	90.1(2)
I(2)–Bi–O(2)	88.7(2)	I(2)–Bi–O(3)	89.1(2)
I(2)–Bi–O(4)	93.1(2)	O(1)–Bi–O(2)	88.3(3)
O(1)–Bi–O(3)	176.5(3)	O(1)–Bi–O(4)	90.8(3)
O(2)–Bi–O(3)	88.3(4)	O(2)–Bi–O(4)	178.0(3)
O(3)–Bi–O(4)	92.6(4)	Bi–O(1)–P(1)	157.6(5)
Bi–O(2)–P(2)	158.0(5)	Bi–O(3)–P(3)	153.0(6)
Bi–O(4)–P(4)	164.9(6)		

formed. Analytical data for the dark orange crystals indicated the presence of considerably more than one hmpa ligand per bismuth, and the structure was established by X-ray crystallography which revealed an ionic material with the composition $[BiI_2(hmpa)_4][I_3]$ **14**. This formula was consistent with the microanalytical data on bulk samples. The cation of **14**, $[BiI_2(hmpa)_4]^+$ (hereafter **14a**), is shown in Fig. 4 and selected bond lengths and angles are listed in Table 3 with atomic positional parameters presented in Table 4. The structure of **14a** is mononuclear with a single bismuth centre co-ordinated to two iodine atoms and four hmpa ligands with an octahedral geometry in which the iodines are *trans* (structure type **H**). The Bi–I (av. 3.051 Å) and Bi–O (av. 2.331 Å) distances are unexceptional and similar to the corresponding distances encountered in **11**, and none of the interbond angles about the bismuth centre deviates from 90 or 180° by more than 3.5° which implies a lone pair with no appreciable stereochemical consequences.

Compound **14** is, to the best of our knowledge, the only structurally characterised example of a class defined by the general formula $[BiX_2(L)_4]^+$ where X is halide and L is a two-electron donor ligand, although a complex formulated as $[BiCl_2(MeCN)_4][SbCl_6]$ (on the basis of spectroscopic and analytical data) has been reported.[14] Cations of this general composition are, however, known for indium and gallium, and we note the structures of two such complexes, $[InI_2(dmso)_4][InI_4]$ **15** (dmso = dimethyl sulfoxide)[15] and $[GaCl_2(bipy)_2][GaCl_4]$ **16** (bipy = 2,2′-bipyridyl).[16] In **15** and **16** the indium and gallium atoms respectively are octahedrally co-ordinated, but in both cases the halides atoms are *cis* as shown in **J**. The essential difference between the cations in **15** or **16** and in **14** is

Table 4 Atomic coordinates (× 10^4) for **14**

Atom	*x*	*y*	*z*
Bi	2528.7(2)	5068.3(3)	1384.3(2)
I(1)	2740.4(4)	3239.4(5)	1530.5(4)
I(2)	2332.8(4)	6873.7(5)	1173.0(5)
O(1)	1855(3)	4947(5)	1597(4)
P(1)	1415.6(13)	5212(2)	1676(2)
N(11)	1516(4)	6086(4)	2005(4)
N(12)	1331(4)	4550(4)	2097(4)
N(13)	921(3)	5278(6)	1045(3)
C(11)	1132(6)	6701(8)	1862(11)
C(12)	2003(5)	6328(9)	2473(7)
C(13)	1074(11)	4735(8)	2456(12)
C(14)	1399(6)	3676(4)	2041(7)
C(15)	447(4)	4919(16)	934(9)
C(16)	895(5)	5808(13)	557(6)
O(2)	1990(4)	4852(5)	387(4)
P(2)	1687.8(14)	4388(2)	−173.2(15)
N(21)	1459(4)	3565(4)	−56(5)
N(22)	1243(3)	4972(4)	−609(4)
N(23)	2027(3)	4157(6)	−499(4)
C(21)	1479(9)	2785(5)	−325(10)
C(22)	1248(8)	3522(9)	366(8)
C(23)	765(4)	4671(8)	−1064(7)
C(24)	1318(5)	5844(5)	−668(7)
C(25)	1844(7)	4163(18)	−1150(4)
C(26)	2523(4)	3807(11)	−169(6)
O(3)	3164(4)	5194(5)	1110(5)
P(3)	3551.2(13)	5661(2)	1032(2)
N(31)	3296(3)	6260(7)	456(4)
N(32)	3901(4)	5032(5)	900(7)
N(33)	3915(5)	6220(7)	1597(4)
C(31)	3577(11)	6901(34)	341(21)
C(32)	2804(4)	6123(10)	−36(5)
C(33)	3905(7)	4162(5)	1004(10)
C(34)	4284(15)	5311(10)	738(26)
C(35)	3745(8)	6952(19)	1772(18)
C(36)	4432(6)	6010(15)	1981(11)
O(4)	3071(3)	5243(5)	2409(4)
P(4)	3372.0(12)	5134(2)	3068.5(15)
N(41)	3944(2)	4998(5)	3225(4)
N(42)	3324(3)	5935(4)	3411(4)
N(43)	3186(3)	4361(4)	3311(4)
C(41)	4094(4)	4415(12)	2893(7)
C(42)	4359(3)	5335(11)	3756(8)
C(43)	3382(8)	5927(7)	4026(5)
C(44)	3357(6)	6758(4)	3200(6)
C(45)	3517(5)	3747(12)	3711(13)
C(46)	2658(3)	4178(9)	3094(8)
I(3)	48.0(9)	2111(2)	−755.7(15)
I(4)	17.2(7)	2388.8(12)	402.5(15)
I(5)	−4.6(8)	2689(2)	1527.7(12)
I(6)	21.5(11)	1851(2)	−229(2)
I(7)	−6.7(8)	2564.8(14)	836(2)
I(8)	−29.8(9)	3229(2)	1902.6(14)

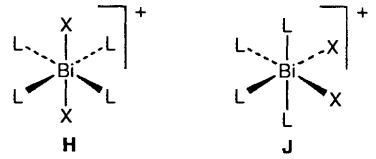

H **J**

an extra two valence electrons present in the latter, and it is possible that the observed structural differences have an electronic origin and are a significant and defining feature for Group 13 and 15 species of the form $[EX_2(L)_4]^+$. The cation in **15** is certainly a good comparison with **14a** in view of the similarity of the ligands L whereas in **16** the bipy ligands may tend to avoid being in the same plane for steric reasons thereby forcing a *cis* dihalide geometry.

In seeking an explanation for this feature, we note first that, in the absence of π effects, the hypothetical unligated cations EX_2^+ should be linear when E is a Group 13 element, since there

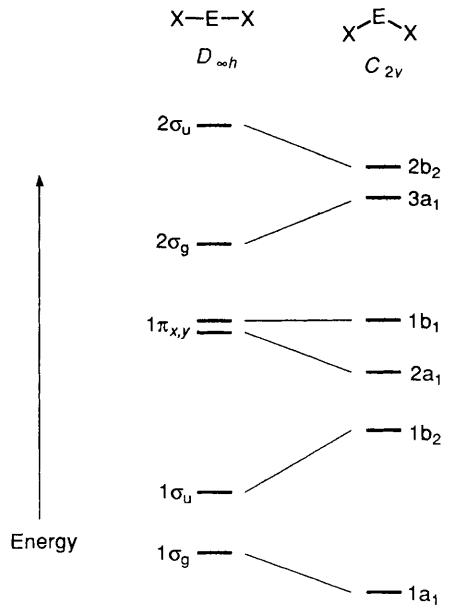

Scheme 1 A correlation diagram between the molecular orbital energy levels of linear and bent EX_2 derived from Fig. 7.3 in ref. 17. Diagrams of the relevant orbitals are also to be found in ref. 17

would be only four valence electrons, whereas a bent structure would be expected for a six-electron cation when E is a Group 15 element; in both cases, the opposite structure is found for the tetraligated cations. Further insight can be obtained if we consider a molecular orbital diagram (σ only) for EX_2 as shown in Scheme 1.

Scheme 1 is derived from Fig. 7.3 in ref. 17 and is a standard, qualitative correlation diagram showing how the energies of the σ molecular orbitals of a EX_2 species change on moving from linear ($D_{\infty h}$) to bent (C_{2v}) EX_2. This diagram can, of course, be used as a basis for rationalising the linear *vs.* bent geometries for unligated four- and six-electron EX_2^+ mentioned above,[17] but it may also be employed to provide some insight into the structural preferences of the tetraligated cations. If we consider a linear EX_2^+ group, the degenerate p orbitals ($1\pi_x$ and $1\pi_y$ which are simply unhybridised p orbitals in this case) have the correct orientation to overlap with the ligand σ orbitals. In fact each p orbital will participate in a three-orbital, four-electron interaction with two mutually *trans* ligand σ orbitals of which only the bonding orbital (as opposed to the filled non-bonding orbital) has a contribution from the E centre. This is shown schematically in Scheme 2 for an electropositive element E and relatively electronegative ligands L. As such, each *trans* pair of ligands effectively donates a pair of electrons to the E centre. For a Group 15 element EX_2^+ species there are an additional six valence electrons to be accommodated which means that the molecular orbitals on the left in Scheme 1 (linear EX_2, $D_{\infty h}$) are filled up to and including $2\sigma_g$. This effective electron count of ten will thus clearly favour a linear rather than a bent EX_2 geometry assuming that the energy of the highest occupied molecular orbital ($2\sigma_g$ *vs.* $3a_1$ in Scheme 1) is the determining factor. In the analogous situation for a Group 13 complex, there are two fewer electrons at the E centre which, for a linear geometry, would fill up to and including $1\pi_{x,y}$. Since a bent geometry lifts the degeneracy and lowers the energy of one of these orbitals (becoming $2a_1$ in C_{2v}), we would therefore anticipate that a bent structure might be the more stable for a Group 13 complex.

Clearly this model is an oversimplification in that we have ignored the energy changes in the other orbitals, any ligand π effects, and, in particular, the effect of the geometry change on the element–ligand σ bonding (and non-bonding) orbitals. Specifically, we have ignored the fact that the non-bonding orbital in Scheme 2 has the correct symmetry to overlap with $2\sigma_g$ but this is unlikely to be important since, to a first

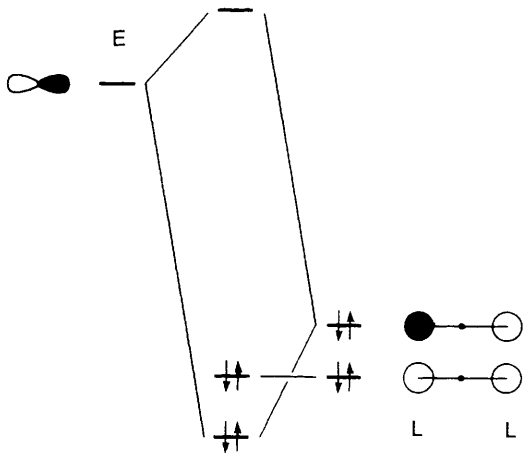

Scheme 2 A three-centre interaction diagram for an electropositive element E showing the interaction of the ligand σ orbitals with a E p orbital

approximation, the interaction is unaffected by a change in angle and it is also likely to be relatively weak for a fairly electropositive E and electronegative ligands L. The distinction between X and L in this argument is also rather arbitrary, but is probably reasonable in view of the similarity in electronegativities between Bi or In and I. Steric effects, which should favour a *trans* type **H** geometry for bulky ligands, have also been ignored, but the model does provide us with, at least, a first step in understanding the structural differences in the complexes described. If the model is reasonable, we expect that the observed differences are likely to be general, but many more examples will be needed before any confidence is justified.

In concluding this section, we draw attention to some other structures which incorporate a BiX_2^+ cation. The only example of a compound of the general formula $[BiX_2(L)_3]^+$ is found in the structure of $[Bi_2(\mu\text{-}Cl)_2Cl_2(tu)_6][BiCl_5(tu)]$[18] wherein a species of this type is present as a dimeric dication. The particular structure adopted is centrosymmetric with two bridging chlorides and with the three ligands on each bismuth centre in a *fac* arrangement as shown in **K**. Four-co-ordinate

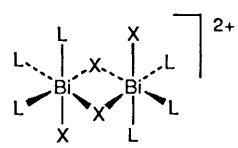

K

complexes of the type $[BiX_2(L)_2]^+$ where X is halide have not yet been structurally characterised, but the closely related complexes $[BiX_2(18\text{-crown-6})]^+$ (18-crown-6 = 1,4,7,10,13,16-hexaoxacyclooctadecane; X = Cl or Br) are known in which two of the 18-crown-6 oxygens are much closer to the bismuth than the other four;[19] the Cl–Bi–Cl angle in this case is 91.0(2)° but this is undoubtedly constrained to a large extent by the nature of the crown ether ligand.

As mentioned above, in the reactions carried out in thf, small amounts of a black crystalline product were also obtained. The attempted determination of the structure of this material by X-ray crystallography was thwarted by disorder problems, and it was not even possible unambiguously to establish a space group. However, it was clear from the partial solution which was possible that this material probably contained the same cation as found in **14** (*i.e.* **14a**). The nature of the anion was not clear from the X-ray data except in so far as the volume of the unit cell, together with the microanalytical data, was consistent with the formula $[BiI_2(hmpa)_4][I_5]$ **17**. Further confirmation of

Table 5 EXAFS analysis: details of final models[a]

N_n[b]	n	r_n/Å	a_n/Å^2	
(*a*) Solid **17**				
4	O	2.277(4)	0.012(1)	k_{max} = 11.0 Å^{-1}
2	I	3.075(8)	0.013(1)	
2	P	3.379(8)	0.002(1)	
2	P	3.818(8)	0.007(2)	R = 0.075
8	N	4.268(24)	0.039(8)	R' = 0.045
4	N	4.748(18)	0.010(4)	
Correlations >0.5: $E_0 - r_1$ −0.783 $r_2 - a_3$ −0.857 $r_3 - a_2$ 0.697				
(*b*) **17** in thf solution				
2	I	2.887(3)	0.014(1)	k_{max} = 12.5 Å^{-1}
1	O	2.589(22)	0.024(6)	R = 0.20
1	P	3.570(9)	0.015(1)	R' = 0.09
Correlations >0.5: $E_0 - r_1$ −0.788				

[a] The estimated standard deviation in the least significant digit as calculated by EXCURV92 model fitting is given in parentheses, here and throughout this paper. We note that such estimates of precision are likely to be underestimates of accuracy and particularly so in cases of high correlation between parameters (see footnote *b*). Residual index $R = \Sigma_i\{k^3(\chi^{obs}_i - \chi^{calc}_i)\}^2/\Sigma_i\{k^3\chi^{obs}_i\}^2$; R' was calculated as for R, with final model parameters, but with data Fourier filtered with r_{max} = 6 Å to remove noise. [b] 'Co-ordination' numbers, N_n (*i.e.* the number of contacts in a given shell), were initially assigned on chemical grounds and then fixed at nearest integral values after refinement.

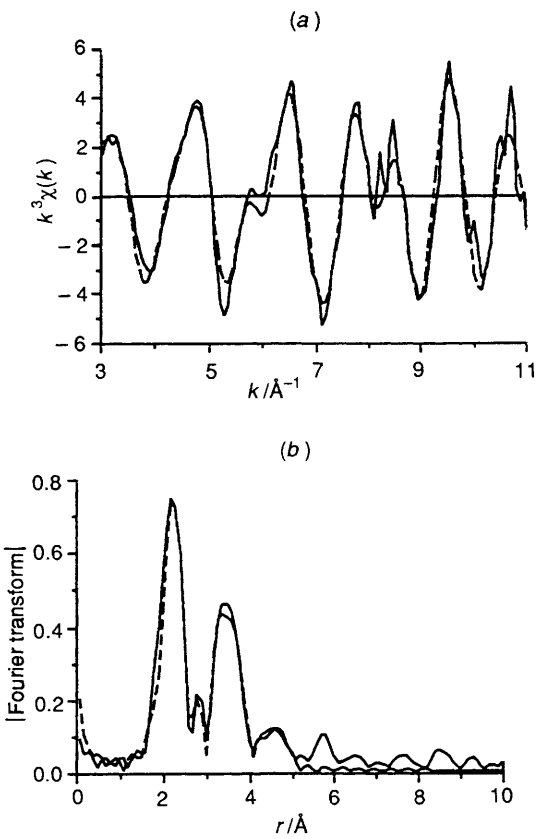

Fig. 5 (*a*) Observed (——) and calculated (– – – –) k^3-weighted Bi L_{III}-edge EXAFS spectrum for solid **17**. (*b*) Observed (——) and calculated (– – – –) Fourier-transform magnitudes (quasi-radial distribution function) of the k^3-weighted Bi L_{III}-edge EXAFS spectrum for solid **17**

the presence of the cation **14a** was obtained from the solid-state Bi extended X-ray absorption fine structure (EXAFS) data.

Transmission EXAFS data were collected on the complex **17** both in the solid state and in thf solution, as described in the Experimental section, and the results of the EXAFS data analyses are summarised in Table 5. Typical Fourier-transform (quasi-radial distribution function) and EXAFS function plots are shown in Figs. 5 and 6.

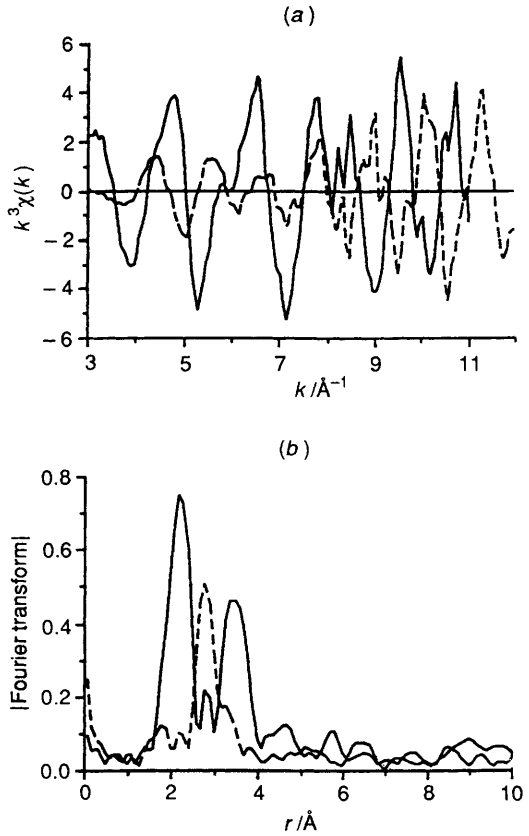

Fig. 6 (*a*) Observed k^3-weighted Bi L_{III}-edge EXAFS spectra for **17** as solid (——) and in thf solution (– – – –). (*b*) Fourier-transform magnitudes (quasi-radial distribution function) of k^3-weighted Bi L_{III}-edge EXAFS spectra for **17** as solid (——) and in thf solution (– – – –)

The Bi L_{III} EXAFS spectrum of **17** in the solid state is fully consistent with the bismuth environment being essentially identical to that observed in the crystal structure analysis of **14**. Thus the crystallographic Bi–I distances in **14** are 3.034(2) and 3.069(2) Å (mean 3.051 Å) which compare well with the value of 3.075(8) Å derived from the EXAFS study of solid **17** although the Bi–O distances in **14** (average 2.331 Å) are slightly longer than those from the EXAFS analysis [2.277(4) Å]. The EXAFS model fitting yielded two Bi···P distances [3.379(8) and 3.818(8) Å] which are comparable to the crystallographic values of 3.72, 3.73, 3.77 and 3.81 Å in **14** (mean 3.76 Å). Finally, two outer shells of atoms modelled as nitrogen [at 4.27(3) and 4.75(2) Å] complete the EXAFS model. Two shells are required to model satisfactorily the rather broad peak at around 3.5 Å in the pseudo-radial distribution function associated with Bi···P distances (see Fig. 5). The rather unrealistically small a (Debye–Waller) values arising from the least-squares fit for these distances are probably a reflection of Bi···O···P multiple scattering (Bi–O–P angles are >150° in **14**) which was not included in the model refined because current codes do not allow for two outer shells involving multiple scattering off a single inner shell. The 'nitrogen' shells are undoubtedly really due to a mixture of nitrogen and carbon atoms at distances between 4 and 5 Å (in **14** Bi···N distances lie between 4.3 and 4.8 Å and Bi···C between 4.3 and 6.2 Å).

On dissolution of **17** in thf substantial changes occur in the EXAFS spectrum (see Fig. 6). In the model fitting these changes can be seen to be associated with the contraction of the Bi–I distance [to 2.887(3) Å] together with a single rather extended Bi–O contact of 2.59(2) Å. In addition the large feature at

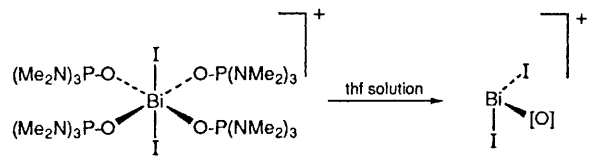

Scheme 3 [O] = unspecified oxygen donor (probably hmpa)

around 3.5 Å in the pseudo-radial distribution function for solid **17** is greatly diminished in thf solution. This is further evidence for the dissociation of most or all of the hmpa ligands [see Scheme 3]. Whether the Bi • • • O contact is due to hmpa or thf co-ordination is not clear, but the best model fitted (Table 5) incorporated a third shell containing one phosphorus atom at 3.57(1) Å, as would be expected if just one hmpa remained co-ordinated in this solution. The reduction in the Bi–I distance is consistent with a change in bismuth co-ordination in which the iodines are no longer *trans* to a strongly bound iodine (or anything else!), *cf.* the Bi–I(3) distance of 2.878(1) Å in **11**.

In conclusion, we note that the reaction between BiI_3 and hmpa in toluene affords the neutral complex **11** as the major product together with smaller yields of **13** when the amount of hmpa is increased. In thf solution, the ionic complexes **14** and **17** are also formed in addition to **11** and probably **13** although the latter species was not detected in this case. The formation of ionic species in thf is not surprising although the presence of the I_3^- and I_5^- anions in **14** and **17** respectively is not readily explained in terms of a straightforward reaction between BiI_3 and hmpa. However, the known photosensitivity of BiI_3 (particularly in solution) is a likely source of diiodine, I_2, with which any substituted iodide, I^-, would probably react thereby affording the observed polyiodide anions. Consistent with this view, we have noted that an initial purple colouration is sometimes observed when samples of BiI_3 are dissolved in thf. Moreover, solvent diffusion of hexane into solutions of pure **11** (obtained from BiI_3 and hmpa in toluene) in thf (which afforded X-ray quality crystals of this complex) also resulted in the formation of compounds **14** and **17**. This observation, together with the solution EXAFS data for **17**, clearly indicates that the nature of the species present in solution can be quite different to those observed in the solid state as a result of the lability of the ligands; a feature which is undoubtedly characteristic of this area of chemistry.*

We also examined the reaction between SbI_3 and hmpa in thf solution. In reactions involving one, two and three equivalents of hmpa to SbI_3, the same pale orange crystalline material was obtained, microanalytical data for which were consistent with the formula $[Sb_2I_6(hmpa)_3]$ **18**. Crystals of **18** were not suitable for X-ray diffraction but a possible structure is of type **C** analogous to **10**. An ionic structure involving polyiodide anions is considered unlikely in view of the pale colour of **18**; the dark colours of **14** and **17** are most likely due to the presence of I_3^- and I_5^- respectively. Moreover, SbI_3 is less photosensitive than BiI_3 making the production of I_2 less likely.

Experimental

General.—All reactions were performed using standard Schlenk techniques under an atmosphere of dry, oxygen-free dinitrogen. All solvents were distilled from appropriate drying agents immediately prior to use (sodium–benzophenone for thf, Et_2O, toluene and hexanes; CaH_2 for CH_2Cl_2). Bismuth triiodide (99%+) and hmpa were procured commercially and used without further purification. Electron-impact mass spectra were obtained on a Kratos MS 80 spectrometer and microanalytical data were obtained at The University of Newcastle.

Preparations.—$[Bi_2I_6(hmpa)_2]$ **11**. The compound hmpa (0.13 cm^3, 0.75 mmol) was added dropwise to an orange solution of BiI_3 (0.441 g, 0.747 mmol) in toluene (20 cm^3) and the mixture was stirred overnight. This resulted in the formation of an orange precipitate of **11**. The supernatant liquid, which was also orange, was removed by syringe and the orange precipitate of **11** was washed with hexane (0.252 g, 42% based on bismuth). X-Ray quality crystals were obtained by solvent diffusion of hexane into thf solutions of **11** at −30 °C (quantities of **14** and **17** were also formed) [Found for $BiI_3(hmpa)$ **11**: C, 9.65; H, 2.25; N, 5.40. $C_6H_{18}BiI_3N_3OP$ requires C, 9.35; H, 2.35; N, 5.45%].

An analogous reaction between BiI_3 (0.542 g, 0.919 mmol) and five equivalents of hmpa (0.80 cm^3, 4.60 mmol) in toluene (20 cm^3) also afforded an orange precipitate and an orange supernatant liquid. The supernatant was removed to a separate flask and fresh toluene (10 cm^3) was added to the precipitate and warmed until most of it had dissolved. This solution was combined with the supernatant liquid and an overlayer of Et_2O (30 cm^3) was added. Solvent diffusion at −30 °C over a period of days afforded an orange oil. This oil was redissolved in CH_2Cl_2 (5 cm^3) and hexane (15 cm^3) was added as an overlayer. Solvent diffusion over a period of days at room temperature afforded a mixture of orange crystalline **11**, as the major product, and yellow **13** (combined weight, 0.422 g) [Found for $BiI_3(hmpa)_2$ **13**: C, 15.25; H, 3.75; N, 8.70. $C_{12}H_{36}BiI_3N_6O_2P_2$ requires C, 15.20; H, 3.85; N, 8.85%].

The reaction between BiI_3 and one equivalent of hmpa in thf (20 cm^3) also afforded an orange solution although no precipitate was formed. Solvent diffusion from an overlayer of hexane (30 cm^3) afforded an intimate mixture of orange crystals of **11**, dark orange crystals of **14** and black crystals of **17**. The amounts of **11**, **14** and **17** formed are probably dependent on the reaction time and the concentration of the reactants in solution. Fully reproducible yields and ratios of **11** to **14** to **17** were rarely obtained.

$[BiI_2(hmpa)_4][I_3]$ **14**. The compound hmpa (0.9 cm^3, *ca.* 5.2 mmol) was added dropwise to a solution of BiI_3 (0.607 g, 1.029 mmol) in thf (30 cm^3) and the resulting orange solution was allowed to stir overnight. After this time the solvent volume was reduced by vacuum to about 10 cm^3 and hexane (20 cm^3) was added as an overlayer. Solvent diffusion over a period of days at −30 °C afforded a large crop of dark orange crystals of **14** as the major crystalline product with smaller quantities of black crystals of **17** also present. Since these two crystalline products were present as an intimate mixture, an accurate yield could not be obtained {Found for $[BiI_2(hmpa)_4][I_3]$ **14**: C, 19.50; H, 4.35; N, 10.30. $C_{24}H_{72}BiI_5N_{12}O_4P_4$ requires C, 18.50; H, 4.65; N, 10.75%; mass spectrum, *m/z* 1002, *P* − hmpa [*P* = $BiI_2(hmpa)_4$]; 822, *P* − 2hmpa; 642, *P* − 3hmpa; 516 *P* − 3hmpa − I; 389, *P* − 3hmpa − 2I. Found for $[BiI_2(hmpa)_4][I_5]$ **17**: C, 16.10; H, 3.95; N, 9.20. $C_{24}H_{72}BiI_7N_{12}O_4P_4$ requires C, 15.90; H, 4.00; N, 9.25%}.

$[Sb_2I_6(hmpa)_3]$ **18**. The compound hmpa (0.45 cm^3, 2.55 mmol) was added dropwise to a solution of SbI_3 (0.640 g, 1.274 mmol) in thf (10 cm^3) which resulted in a yellow-brown solution which was allowed to stir overnight leading to a slight lightening of the colour. The solvent volume was reduced to about 5 cm^3 by vacuum and an overlayer of hexane (20 cm^3) was added. Solvent diffusion over a period of days at −30 °C afforded pale orange crystalline **18** (75%). Better quality crystals were obtained by solvent diffusion at room temperature but these were still not suitable for X-ray crystallography {Found for $[Sb_2I_6(hmpa)_3]$ **18**: C, 14.40; H, 3.25; N, 8.10. $C_{18}H_{54}I_6N_9O_3P_3Sb_2$ requires C, 14.00; H, 3.55; N, 8.20%}.

* With this point in mind, it is worth noting that solution spectroscopic data, such as infrared and NMR, are of little diagnostic use; the compounds described herein are very much solid-state materials and do not maintain their integrity in solution. Solid-state infrared spectra are also uninformative from a structural point of view although solid-state ^{31}P NMR spectroscopy might be more useful.

X-Ray Crystallography.—*Crystal data for compound* **11**. $C_{12}H_{36}Bi_2I_6N_6O_2P_2$, M = 1537.8, monoclinic, space group $P2_1/n$, a = 7.7610(8), b = 11.5695(7), c = 19.771(2) Å, β = 97.926(7)°, U = 1758.3(3) Å^3, Z = 2, D_c = 2.90 g cm^{-3}, $F(000)$ = 1360, λ = 0.710 69 Å, μ(Mo-Kα) = 15.29 cm^{-1}, T = 298 K.

Data collection and reduction. An orange crystal of approximate dimensions 0.37 × 0.16 × 0.20 mm was mounted on a glass fibre and coated in acrylic resin to prevent decomposition in air. Data were collected using the ω–2θ scan mode on a CAD4F automated diffractometer using graphite monochromated Mo-Kα radiation. Unit-cell parameters were determined by refinement of the setting angles (11 < θ < 13°) of 25 reflections, using the SET4 routine which averages angles from four diffracting positions. A linear correction was applied for an observed decay of *ca.* 2% in the intensities of three standard reflections, together with standard Lorentz, polarisation and absorption/extinction (DIFABS;[20] maximum, minimum corrections 1.70 and 0.71 respectively) corrections. A total of 3498 measured reflections (θ range 2–25°, h 0–9, k 0–13, l −23 to 23) yielded 3067 independent data of which 2311 reflections having an intensity greater than 3.0 $\sigma(I)$ were considered observed and used in structure determination.

Structure solution and refinement. The structure was solved by direct methods (MITHRIL[21]) and subsequent electron-density difference syntheses. Refinement was by full-matrix least squares minimising the function $\Sigma w(|F_o| - |F_c|)^2$ with the weighting scheme $w = [\sigma^2(F_o)]^{-1}$; $\sigma(F_o)$ was estimated from counting statistics. All non-H atoms were allowed anisotropic thermal motion. The H atoms were included at calculated positions (C–H 1.0 Å) and were allowed to ride on their attached C atom. A common refined isotropic thermal parameter was used for all H atoms. Refinement using a total of 137 parameters converged at $R(R')$ = 0.033 (0.038) with mean and maximum Δ/σ values of 0.01 and 0.058 respectively in the final cycle. A final electron-density difference synthesis showed no peaks of chemical significance (maximum $\Delta\rho$ = +1.64, minimum $\Delta\rho$ = −1.36 e Å^{-3} in the vicinity of the Bi atom). The e.s.d. of an observation of unit weight (S) was 1.79. Neutral-atom scattering factors were taken from ref. 22 with corrections applied for anomalous scattering. All calculations were carried out on a MicroVAX 3600 computer using the Glasgow GX suite of programs.[23]

Crystal data for compound **14**. $C_{24}H_{72}BiI_5N_{12}O_4P_4$, M = 1560.30, monoclinic, space group $C2/c$, a = 30.314(7), b = 16.484(6), c = 24.984(6) Å, β = 116.97(2)°, U = 11 127(6) Å^3, Z = 8, D_c = 1.863 g cm^{-3}, $F(000)$ = 5920, λ = 0.710 73 Å, μ(Mo-Kα) = 6.095 mm^{-1}, T = 160 K.

Data collection and reduction. A dark orange crystal of approximate dimensions 0.44 × 0.40 × 0.40 mm was mounted on a glass fibre and coated with perfluoropolyether oil, which acted as both adhesive and protective coating at 160 K. Data were collected using the ω–θ scan mode and on-line profile fitting[24] on a Stoe-Siemens diffractometer with graphite monochromated Mo-Kα radiation and a Cryostream cooler.[25] Unit-cell parameters were refined from θ values (10.3–11.3°) of 32 reflections measured at ± ω. Standard Lorentz, polarisation, linear decay (*ca.* 1% based on five standard reflections) and semi-empirical absorption corrections (ellipsoid model, transmission 0.357–0.474) were applied. A total of 7312 measured reflections (θ range 2.5–22.5°, h 0–24, k −17 to 0, l −26 to 24 together with some equivalent reflections) yielded 7189 independent data (R_{int} = 0.0157), all of which were used in structure determination except for 18 reflections recorded with large negative net intensities.

Structure solution and refinement. The structure was solved by heavy-atom methods. Refinement was by full-matrix least squares minimising the function $\Sigma w(F_o^2 - F_c^2)^2$ with weighting $w^{-1} = \sigma^2(F_o^2) + (0.0723P)^2 + 343.15P$, where $P = (F_o^2 + 2F_c^2)/3$. Anisotropic displacement parameters were refined; H atoms were not included. The I_3^- anion was found to be disordered [53.3:46.7(3)%] over two overlapping sites, which were successfully refined. Similarity restraints were applied to the hmpa ligands. For a total of 480 parameters, $wR2 = [\Sigma w(F_o^2 - F_c^2)^2/\Sigma w(F_o^2)^2]^{\frac{1}{2}} = 0.1876$ for all 7171 data, S = 1.110, and conventional R = 0.0503 based on F values for 5581 reflections having $F_o^2 > 2\sigma(F_o^2)$; maximum Δ/σ = 0.004, maximum $\Delta\rho$ = +2.21, minimum $\Delta\rho$ = −1.58 e Å^{-3}. Scattering factors, embedded in the refinement program, were taken from ref. 26. Calculations were carried out with programs of the SHELX family.[27]

Additional material available from the Cambridge Crystallographic Data Centre comprises H-atom coordinates, thermal parameters and remaining bond lengths and angles.

EXAFS.—All EXAFS data were collected at the Daresbury SRS on station 7.1 in transmission mode, using samples prepared in a glove-box under nitrogen. The solid sample was of *ca.* 1 mm thickness and was diluted in boron nitride in order to achieve change in $\log(I_0/I)$ in the range 1–2 at the absorption edge. Solution spectra were measured in a cell of thickness *ca.* 3 mm and summed to provide the data to be analysed. Raw data were corrected for dark currents and converted to k-space (with EXCALIB[28]), and backgrounds subtracted (with EXBACK[28]) to yield EXAFS functions $\chi^{obs}{}_i(k)$. These were Fourier filtered to remove features at distances below *ca.* 1.2 Å but *not* to remove long distance features of the quasi-radial distribution function (*i.e.* no noise removal was attempted). Model fitting was carried out with EXCURV 92,[28] using curved wave theory. Only shells significant at the 99% level[29] were included in final models, *i.e.* shells added to the model caused reduction in the R indices by > 6% of their previous value. Details of the final models employed are listed in Table 5, which gives interatomic distances (r_n), Debye–Waller factors (a_n) and the 'co-ordination' numbers (N), *i.e.* the numbers of atoms in a given shell n. *Ab initio* phase shifts and back-scattering factors using spherical wave theory with 25 l values were used throughout. The values used throughout for the proportion of absorption leading to EXAFS ('AFAC' = 0.8) and the magnitude of inelastic effects modelled by an imaginary potential ('VPI' = −4.0 eV), were confirmed by fits to data reported previously.[12,30]

Acknowledgements

We thank the SERC for financial support and for two studentships (to N. L. P. and S. E. S.) and the staff of the Daresbury SRS for technical support. N. C. N. also thanks the Royal Society for additional supporting funds.

References

1 G. A. Fisher and N. C. Norman, unpublished work.
2 L. P. Battaglia, A. Bonamartini Corradi, G. Pelizzi and M. E. Vidoni Tani, *J. Chem. Soc., Dalton Trans.*, 1977, 1141.
3 L. P. Battaglia and A. Bonamartini Corradi, *J. Chem. Soc., Dalton Trans.*, 1981, 23.
4 L. P. Battaglia, A. Bonamartini Corradi, M. Nardelli and M. E. Vidoni Tani, *J. Chem. Soc., Dalton Trans.*, 1978, 583.
5 L. P. Battaglia and A. Bonamartini Corradi, *J. Chem. Soc., Dalton Trans.*, 1983, 2425.
6 L. P. Battaglia, A. Bonamartini Corradi and G. Pelosi, *J. Crystallogr. Spectrosc. Res.*, 1992, **22**, 275.
7 W. Clegg, R. J. Errington, R. J. Flynn, M. E. Green, D. C. R. Hockless, N. C. Norman, V. C. Gibson and K. Tavakkoli, *J. Chem. Soc., Dalton Trans.*, 1992, 1753.
8 F. Lazarini and S. Milicev, *Acta Crystallogr., Sect. B*, 1976, **32**, 2873.
9 F. Lazarini, L. Golic and G. Pelizzi, *J. Cryst. Mol. Struct.*, 1976, **6**, 113.
10 W. Clegg, R. J. Errington, G. A. Fisher, D. C. R. Hockless, N. C. Norman, A. G. Orpen and S. E. Stratford, *J. Chem. Soc., Dalton Trans.*, 1992, 1967.
11 W. Clegg, R. J. Errington, G. A. Fisher, R. J. Flynn and N. C. Norman, *J. Chem. Soc., Dalton Trans.*, 1993, 637.
12 W. Clegg, N. A. Compton, R. J. Errington, G. A. Fisher, D. C. R. Hockless, N. C. Norman, N. A. L. Williams, S. E. Stratford, S. J.

Nichols, P. S. Jarrett and A. G. Orpen, *J. Chem. Soc., Dalton Trans.*, 1992, 193.
13 S. Pohl, W. Saak, R. Lotz and D. Haase, *Z. Naturforsch., Teil B*, 1990, **45**, 1355.
14 G. R. Willey, H. Collins and M. G. B. Drew, *J. Chem. Soc., Dalton Trans.*, 1991, 961.
15 F. W. B. Einstein and D. G. Tuck, *Chem. Commun.*, 1970, 1182.
16 R. Restivo and G. J. Palenik, *Chem. Commun.*, 1969, 867.
17 T. A. Albright, J. K. Burdett and M. H. Whangbo, *Orbital Interactions in Chemistry*, Wiley, New York, 1985.
18 L. P. Battaglia, A. Bonamartini Corradi, G. Pelizzi and M. E. Vidoni Tani, *Cryst. Struct. Commun.*, 1975, **4**, 399.
19 N. W. Alcock, M. Ravindran and G. R. Willey, *J. Chem. Soc., Chem. Commun.*, 1989, 1063; R. D. Rogers, A. H. Bond, S. Aguinaga and A. Reyes, *J. Am. Chem. Soc.*, 1992, **114**, 2967; see also A. Neuhaus, G. Frenzen, J. Pebler and K. Dehnicke, *Z. Anorg. Allg. Chem.*, 1992, **618**, 93.
20 N. Walker and D. Stuart, *Acta Crystallogr., Sect. A*, 1983, **39**, 158.
21 C. J. Gilmore, *J. Appl. Crystallogr.*, 1984, **17**, 42.
22 *International Tables for X-Ray Crystallography*, Kynoch Press, Birmingham, 1974, vol. 4.
23 P. R. Mallinson and K. W. Muir, *J. Appl. Crystallogr.*, 1985, **18**, 51.
24 W. Clegg, *Acta Crystallogr., Sect. A*, 1981, **37**, 22.
25 J. Cosier and A. M. Glazer, *J. Appl. Crystallogr.*, 1986, **19**, 105.
26 *International Tables for Crystallography*, Kluwer Academic Publishers, Dordrecht, 1992, vol. C, Tables 4.2.6.8 and 6.1.1.4.
27 G. M. Sheldrick, SHELXTL/PC manual, Siemens Analytical X-ray Instruments Inc., Madison, 1990; SHELXL 93, beta test version, University of Göttingen, 1992.
28 N. Binstead, S. J. Gurman and J. W. Campbell, EXCALIB, EXBACK and EXCURV 92, SERC Daresbury Laboratory Programs, 1992.
29 R. W. Joyner, K. J. Martin and P. Meehan, *J. Phys. C*, 1987, **20**, 4005.
30 N. A. Compton, R. J. Errington, G. A. Fisher, N. C. Norman, P. M. Webster, P. S. Jarrett, S. J. Nichols, A. G. Orpen, S. E. Stratford and N. A. L. Williams, *J. Chem. Soc., Dalton Trans.*, 1991, 669.

Received 15*th April* 1993; *Paper* 3/02163G